Biosensors and Bioelectronics 85 (2016) 371–380

Contents lists available at ScienceDirect

Biosensors and Bioelectronics

journal homepage: www.elsevier.com/locate/bios

Fluorescent peptide biosensor for monitoring CDK4/cyclin D kinase activity in melanoma cell extracts, mouse xenografts and skin biopsies

Camille Prével [a], Morgan Pellerano [a], Juan A. González-Vera [a], Pauline Henri [a], Laurent Meunier [a], Julien Vollaire [b,c], Véronique Josserand [b,c], May C. Morris [a,*]

[a] Institut des Biomolécules Max Mousseron, CNRS, UMR 5247, Université de Montpellier, Faculté de Pharmacie, 15, Av. Charles Flahault, 34093 Montpellier, France
[b] INSERM U823, Institut Albert Bonniot, F-38000 Grenoble, France
[c] Universite Grenoble Alpes, Institut Albert Bonniot, F-38000 Grenoble, France

ARTICLE INFO

Article history:
Received 9 February 2016
Received in revised form
15 April 2016
Accepted 18 April 2016
Available online 22 April 2016

Keywords:
Fluorescent biosensor
CDK4/Cyclin D
Kinase activity
Melanoma

ABSTRACT

Melanoma constitutes the most aggressive form of skin cancer, which further metastasizes into a deadly form of cancer. The $p16^{INK4a}$-Cyclin D-CDK4/6-pRb pathway is dysregulated in 90% of melanomas. CDK4/Cyclin D kinase hyperactivation, associated with mutation of CDK4, amplification of Cyclin D or loss of $p16^{INK4a}$ leads to increased risk of developing melanoma. This kinase therefore constitutes a key biomarker in melanoma and an emerging pharmacological target, however there are no tools enabling direct detection or quantification of its activity.

Here we report on the design and application of a fluorescent peptide biosensor to quantify CDK4 activity in melanoma cell extracts, skin biopsies and melanoma xenografts. This biosensor provides sensitive means of comparing CDK4 activity between different melanoma cell lines and further responds to CDK4 downregulation by siRNA or small-molecule inhibitors. By affording means of monitoring CDK4 hyperactivity consequent to cancer-associated molecular alterations in upstream signaling pathways that converge upon this kinase, this biosensor offers an alternative to immunological identification of melanoma-specific biomarkers, thereby constituting an attractive tool for diagnostic purposes, providing complementary functional information to histological analysis, of particular utility for detection of melanoma onset in precancerous lesions. This is indeed the first fluorescent peptide biosensor which has been successfully implemented to monitor kinase activity in skin samples and melanoma tumour xenografts. Moreover by enabling to monitor response to CDK4 inhibitors, this biosensor constitutes an attractive companion assay to identify compounds of therapeutic relevance for melanoma.

1. Introduction

Skin cancers constitute an important cause of death worldwide, with an estimated 80,000 deaths a year as of 2010, 49,000 of which are due to melanoma. This aggressive and invasive form of skin cancer arises from deregulated proliferation of melanocytes, and can metastasize into a deadly form of cancer (Lozano et al., 2012). Several morphological, histological and serological biomarkers currently serve to diagnose malignant melanoma and establish a prognostic profile, including melanocyte lineage and differentiation antigens such as S100-beta, melanoma inhibitory activity (MIA) and tyrosinase, proangiogenic factors such as VEGF (Vascular Endothelial Growth Factor), molecules involved in cell adhesion and motility such as matrix metalloproteinases MMP-1 and 9, cytokines and cytokine receptors IL-6, IL-10 and sIL-2R, HLA molecules and other more general cancer biomarkers including C-reactive protein, albumin and lactate dehydrogenase (Bosserhoff et al., 1997; Guo et al., 1995; Utikal et al., 2007). Histological analysis of skin biopsies constitutes the standard procedure for melanoma diagnostics, but remains poorly standardized, and is not implemented to monitor the onset and early-stage progression of this disease (Taylor, 2000). Moreover, immunohistochemistry and ELISA convey information concerning the presence and relative abundance of biomarkers, but do not translate mutations in pathways that alter enzymatic activities associated with deregulated cell growth and proliferation. Hence, new tools are required to provide complementary information concerning enzymatic biomarkers of interest for diagnostic and prognostic purposes.

More recent genetic, transcriptomic and proteomic profiling studies have led to characterization of the landscape of genomic mutations in cutaneous melanoma, to identification of driver mutations and establishment of a framework for genomic

* Corresponding author.
E-mail address: may.morris@univ-montp1.fr (M.C. Morris).

http://dx.doi.org/10.1016/j.bios.2016.04.050
0956-5663/

classification of melanoma into four subtypes based on the most prevalent significantly mutated genes (Cancer Genome Atlas Network, 2015; Hodis et al., 2012). These studies highlight molecular pathways and targets which offer new perspectives for the development of complementary diagnostic and therapeutic tools. In particular, the cyclin-dependent kinase CDK4 has been identified as an emerging pharmacological target in human melanoma (Mahgoub et al., 2015; Miller and Flaherty, 2014; Sheppard and McArthur, 2013). This serine/threonine kinase associates with D-type cyclins and integrates stimuli that promote exit from quiescence, entry into and progression through G1, through phosphorylation of its substrate, the Retinoblastoma tumour suppressor protein (pRb) (Malumbres and Barbacid, 2009). The $p16^{INK4a}$-Cyclin D-CDK4/6-pRb pathway is dysregulated in 90% of melanomas and CDK4 hyperactivation may occur through various fashions, including mutation of CDK4 (R24C) which prevents binding of the endogenous inhibitor $p16^{INK4a}$, amplification of Cyclin D (18% melanomas), genetic deletion or loss-of-function of its endogenous inhibitor $p16^{INK4a}$ (deletion of CDK2NA in 50–60% metastatic tumours) (Tsao et al., 2012; Young et al., 2014). Moreover in both human and mouse models of melanoma, activation of the CDK4 pathway potently cooperates with mutant BRAF or NRAS in transformation of melanocytes (Chawla et al., 2010) inferring that combination strategies utilizing inhibition of complementary oncogenic pathways may offer a very promising approach (Miller and Flaherty, 2014). Furthermore, recent data suggest that cell cycle inhibition by CDK4 inhibitors sensitizes melanoma cells to compounds that induce apoptosis (Quast et al., 2015). Taken together, these studies identify CDK4/Cyclin D activity as a relevant biomarker of melanoma, and suggest that tools reporting on CDK4 kinase activity and assays enabling quantification of its hyperactivity directly from skin biopsies would offer promising means of identifying the onset of melanoma and monitoring progression of this disease.

In this study we describe a fluorescent peptide biosensor that reports on CDK4/Cyclin D kinase activity through sensitive changes in fluorescence intensity. We show that this biosensor responds to recombinant CDK4/Cyclin D1 and can report on CDK4 activity in melanoma cell extracts, thereby enabling quantification of differences in kinase activity which cannot be identified by simple analysis of protein kinase expression levels, associated with molecular alterations in individual components of the $p16^{INK4a}$-Cyclin D-CDK4/6-pRb pathway. This biosensor further reports on CDK4 kinase inhibition following treatment with small molecule inhibitors or siRNA, thereby allowing to assess their overall efficacy in a physiologically-relevant environment. Finally we show that this technology can be readily implemented to probe CDK4 activity in skin biopsies and in melanoma xenograft lysates, thereby constituting an attractive tool for diagnostics, prediction of pathological progression and response to therapeutics targeting the CDK4 biomarker.

2. Materials and methods

2.1. Design and engineering of CDKACTRb protein biosensor

CDKACTRb was engineered by replacing the substrate sequence of CDKACT derived from histone H1 (Van et al., 2014) by a substrate sequence derived from Rb in which the proline at position −2 relative to the SP phosphorylation site 795 was replaced by a cysteine residue.

The complete sequence of CDKACTRb is as follows:

GEVVDSHLSDMLQQLHSVNASKPSERGLVRQEEAEDPASIPIFWVSKWVDYSDKYGLGYQLSDNSVGVLFNDSTRLILYNDGDSLQYIERDGTESYLTVSSHPNSLMKKITLLKYFRNYMSEHLLKAGANITPREGDELARLPYLRTWFRTRSAIILHLSNGSVQINFFQDHTKLILSPLMAAVTYIDEKRDFRTYRLSLLEEYGSSKELASRLRYARTMVDKLLSSRSASNRLKASEFPGAGGTGLPGGYKFCSSPLRIPG.

GST-CDKACTRb was expressed in *Escherichia coli* BL21pLyS following induction with 0.5 mM IPTG, at 20 °C overnight, then purified on High Performance Glutathione Sepharose (GE Healthcare) in 50 mM TrisHCl, pH 7.4, 150 mM NaCl, and eluted with 50 mM glutathione in the same buffer, followed by gel filtration chromatography on Superdex75 (GE Healthcare) in the same buffer. Following purification, CDKACTRb was labelled with a 10-fold molar excess of Cy3-maleimide, then further purified on NAP5 columns in 50 mM TrisHCl, pH 7.4, 150 mM NaCl, to remove excess label.

2.2. Design and synthesis of CDKACT4 peptide biosensors and derived peptides

Peptides were synthesized by GLS Biochem and purified to 95%.

The long WW peptide was derived from the native WW domain of Pin1 previously described by Anai et al. (2007) to generate a phosphopeptide hybrid biosensor (residues 6–39). The shorter version was derived from the residues that line the interface with the phosphopeptide in the crystal structure of WW Pin1 complexed to a phosphopeptide substrate (PDB 1F8A).

The Rb substrate peptide was derived from the sequence around S795.

WW long	GWEKRMSRSSGRVYYFNHITNASQWERPSG
WW short	GFARVYMSRSSGWERPSGG
Rb substrate	GGYKFCSSPLRIPG
Phospho Rb substrate	GGYKFCSpSPLRIPG
WWRb	GWEKRMSRSSGRVYYFNHITNASQWERPSG GG YKFCSSPLRIPG
CDKACT4	GFARVYMSRSSGWERPSGG YKFCSSPLRIPG

2.3. Protein expression and purification of Cyclin-dependent kinases

Recombinant GST-CDK4, GST-Cyclin D1 and GST-CIV, the CDK-activating kinase of *Saccharomyces cerevisiae*, were expressed in *E. coli* by IPTG induction and purified by chromatography as described previously (Gondeau et al., 2005). GST-CDK4/Cyclin D1 complex was formed following individual purification of each subunit and stoichiometric incubation, then further incubated with GST-CIV to ensure its complete activation.

2.4. Fluorescence titration assays

Fluorescence titration assays were performed in 96-well plates in a thermostated chamber (Polarstar, BMG) at 30 °C in 200 μL phosphate buffer saline with 200 nM concentration of FITC-labelled species (Rb peptide or Rb phosphopeptide). Changes in fluorescence emission were recorded at 520 nm following excitation at 495 nm. Data analysis was performed using the GraFit Software (Erathicus Ltd) and curve fitting was performed using a quadratic equation, as described in (Gondeau et al., 2005).

2.5. Fluorescence kinase assays

Fluorescence kinase assays were performed in 96-well plates in a thermostated chamber (Polarstar, BMG) at 30 °C in 200 μL

phosphate buffer saline supplemented with 5 mM $MgCl_2$, 0.5 mM ATP, except when stated otherwise. Changes in TAMRA and Cy3 fluorescence emission were recorded at 570 nm following excitation at 544 nm. In all experiments, relative fluorescence was calculated following subtraction of CDKACTRb-Cy3 or CDKACT4-TAMRA fluorescence from fluorescence values obtained in the presence of protein kinases, inhibitors or cell extracts. Data analysis was performed using the GraFit Software (Erathicus Ltd). Experiments were performed in triplicate, and error bars indicate standard deviation from average. Histograms represent relative fluorescence intensity values after 5000 s, unless specified otherwise.

2.6. Inhibitors

Roscovitine, PD-0332991, LY2835219, AT7519, H89 and U0126 were purchased from Euromedex. RO3306 was purchased from CalbioChem. PP2 was purchased from Sigma. All stock solutions were made in DMSO and diluted in PBS to the desired concentration freshly prior to use. For animal experiments PD-0332991 was diluted in sodium lactate buffer 50 mM.

2.7. Cell culture and extract preparation

Cell culture media, serum and antibiotics were purchased from Invitrogen. All cell lines were cultured in DMEM/RPMI + Glutamax supplemented with 10% FCS, 100 units/mL penicillin (G sodium salt) and 100 μg/mL streptomycin at 37 °C in an atmosphere containing 5% CO_2.

Melanoma cell lines used in this study:

	CDKN2A	CDK4	Rb	BRAF	NRAS
A375	mutated (E61Stop, Loss of function)	WT	WT	V600E	WT
Mewo	mutated (R80Stop, Loss of function)	WT	WT	WT	WT
SK-MEL2	WT	WT	WT	WT	mutated (Q61R)
SK-MEL28	WT	R24C		V600E	WT

siRNA targeting CDK4 were purchased from Santa Cruz (sc-29261). Internalization of siRNA in cells was performed using CADY peptide (Crombez et al., 2009). Unsynchronized A375 cells were cultured to 60% confluence. A375 cells were treated with complexes of siRNA (100 nM)/CADY (4 μM) (1/40 ratio) for 48 h.

Cell extracts were prepared in PBS lysis buffer containing PBS (Sigma), pH 7.4, 150 mM NaCl, 0.2% NP40, 1 mM EDTA, 2 mM PMSF, CompleteTM protease inhibitors (Roche), and normalized following spectrophotometric dosage at 280 nm.

Fractionation of A375 cell extracts prepared from 5 million cells in 500 μL PBS lysis buffer was performed by gel filtration chromatography on a Superose 6 10/300 GL column (GE Healthcare). 500 μL fractions were collected and 50 μL were used for kinase activity assays.

2.8. Western blotting

Polyclonal rabbit anti-CDK4 antibody was purchased from Santa Cruz (sc-260). Monoclonal mouse α-tubulin antibody was purchased from Amersham (N356). Polyclonal rabbit anti-actin antibody was purchased from Cell Signaling (4967).

2.9. Preparation of extracts from skin biopsies

Epidermis and dermis were separated by addition of thermolysine (0.5 mg/mL diluted in PBS (Sigma)) for 3 h at 37 °C. Total proteins were extracted from frozen skin biopsies in 50 mM Trizma Base, 0.5 M NaCl, 5 mM EDTA, 0.6% NP40 and grinding with an Ultra TurraxTM, then normalized following spectrophotometric dosage at 280 nm.

2.10. A375 xenografts in mice

All animal experiments were conducted in agreement with the Principles of Laboratory Animal Care (National Institutes of Health publication no. 86-23, revised 1985) and approved by the regional ethics committee. Female 6 weeks old NMRI nude mice (Janvier, Le Genest- Isle, France) were anesthetized (isoflurane/oxygen 3.5% for induction and 1.5% thereafter) and 3.10^6 A375 (luciferase-transfected) cells in 200 μL phosphate-buffered saline were implanted subcutaneously into the flank of mice and after 24 days of tumour growth, when tumours had reached $257 \pm 64\ mm^3$, mice were treated daily orally with CDK4 inhibitor 150 mg/kg PD-0332991 for 3 or 7 days, or through intraperitoneal injection with the CDK2,5,7,9 inhibitor Roscovitine at 50 mg/kg for 5 or 11 days. Mice were then sacrificed and tumours were collected and frozen. Total proteins were extracted from tumour samples by addition of a luciferase cell culture lysis reagent (25 mM Tris-phosphate pH 7.8, 2 mM DTT, 2 mM EDTA, 10% glycerol, 1% Triton X-114) and grinding with an Ultra TurraxTM, then normalized to the proportion of cancer cells (A375 luciferase) (Victor^3 V luminescence microplate reader, Perkin Elmer).

3. Results

3.1. Design and Characterization of a CDK4-specific protein biosensor

Although CDK4/Cyclin D kinase constitutes an established biomarker and pharmacological target in melanoma, there are no means of probing its hyperactivity in a sensitive and quantitative fashion. Indeed, the larger part of technologies to probe this kinase activity currently rely on radioactivity or antibody-based approaches. Therefore, in order to probe CDK4/Cyclin D activity, we engineered a CDK4-specific protein biosensor derived from a previously-developed biosensor that responds to overall CDK/Cyclin activity through sensitive changes in fluorescence intensity (Van et al., 2014). CDKACTRb was designed by incorporating a substrate sequence derived from the phosphorylation site of Retinoblastoma protein (Rb) which is specifically phosphorylated by CDK4/Cyclin D (S795) (Grafstrom et al., 1999) with the phosphoamino acid binding domain (PAABD) derived from Polo-box domain of Plk1, devoid of cysteine residues (Van et al., 2014) (Fig. 1A). When CDKACTRb was labelled with a Cy3 dye on the unique cysteine proximal to the phosphorylation site of the Rb substrate sequence, this protein biosensor responded to recombinant CDK4/Cyclin D1 through enhancement of fluorescence emission (20–25%), inferring an intramolecular interaction between the PAABD and the phosphorylated substrate moiety that alters the local environment of the probe, as reported for the generic CDKACT biosensor. Moreover this fluorescence enhancement was significantly reduced upon addition of the CDK4-specific inhibitor PD-0332991 (Fig. 1B). CDKACTRb further reported on endogenous CDK4 activity from A375 melanoma cell extracts in a dose-dependent fashion, since addition of increasing concentrations of PD-0332991 reduced the fluorescent signal of CDKACTRb accordingly (Fig. 1C and D). These results further allowed to

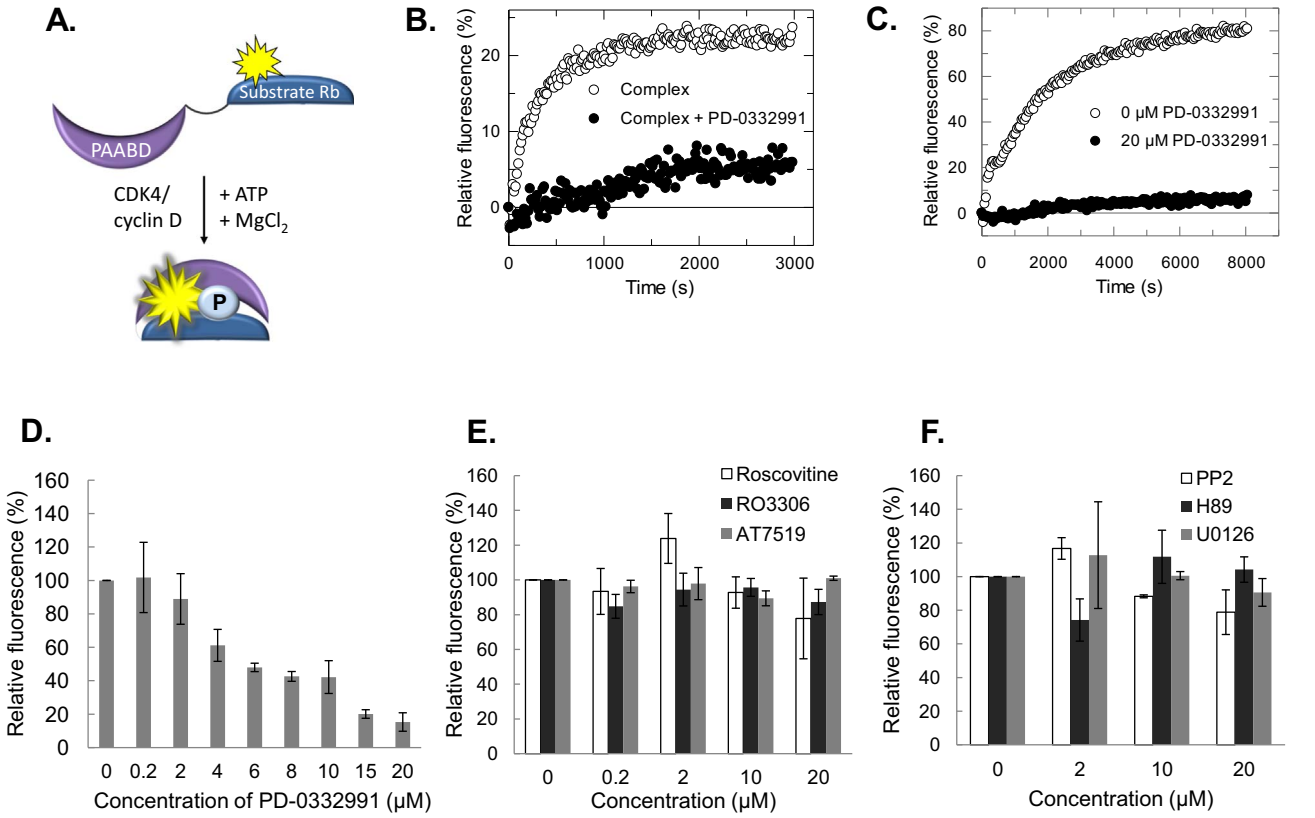

Fig. 1. The CDKACTRb protein biosensor responds specifically to recombinant CDK4/Cyclin D1 and CDK4 activity from melanoma cell extracts. (A) CDKACTRb biosensor consists of a CDK4-specific substrate sequence derived from pRb in which a cysteine residue was introduced at position −2 relative to the SP phosphorylation site (795), and a phospho amino acid-binding domain derived from the PBD of Plk1 (Van et al., 2014) which recognizes the substrate sequence phosphorylated by CDK4/Cyclin D kinase. (B) Fluorescence of 50 nM CDKACTRb-Cy3 was monitored over time upon incubation with 75 nM active recombinant CDK4/Cyclin D1 alone (open circles) and with 20 µM PD-0332991 (black circles). (C) Fluorescence of 25 nM CDKACTRb-Cy3 was monitored over time upon incubation with 10 µg A375 cell extracts ± PD-0332991 alone (open circles) and with 20 µM PD-0332991 (black circles). (D) Fluorescence of 25 nM CDKACTRb-Cy3 was monitored upon incubation with 10 µg A375 cell extracts ± different concentrations of PD-0332991 (CDK4/6 inhibitor), or (E) Roscovitine (CDK1/2/5/7/9 inhibitor), RO3306 (CDK1 inhibitor), AT7519 (CDK2/4/5/9 inhibitor), (F) PP2 (Src inhibitor), U0126 (MAPK inhibitor) or H89 (PKA inhibitor).

determine an IC_{50} value of 5.9 µM for PD-0332991 using A375 melanoma cell extracts (Fig. 1D and Fig. S1), a value which reflects the inhibitory efficiency of this compound in a more physiological context than with the purified recombinant kinase alone. In contrast, other CDK kinase inhibitors (Roscovitine, RO3306, AT7519) and other protein kinase inhibitors (PP2, H89, U0126) had no significant effect on CDKACTRb fluorescence, inferring it responds specifically to CDK4 activity (Fig. 1E and F).

3.2. Development of a CDK4-specific Peptide Biosensor

Preparation of the CDKACTRb protein biosensor requires expression and purification of a recombinant protein scaffold with limited yield and long-term storage, since it suffers from degradation over time. To circumvent this issue, we designed a bipartite modular peptide derivative of CDKACTRb, which can be readily synthesized at a large-scale and stored in a lyophilized form. This peptide derivative (WWRb) bears the same Rb substrate and a short PAABD derived from the WW domain of the prolyl-isomerase Pin1, which was previously used as a phosphorecognition domain in a hybrid biosensor (Anai et al., 2007) (Fig. 2A). However, following labelling of this peptide biosensor on the unique cysteine at position −2 relative to the serine group phosphorylated by CDK4/Cyclin D, we found that it failed to respond in a robust and reproducible fashion (Fig. S2). We hypothesized that this might be due to a lack of proper conformation of the WW domain, and therefore designed a shorter artificial PAABD derived from the interface of the WWdomain of Pin1 with a phosphopeptide substrate. Analysis of the crystal structure of this domain complexed to a phosphopeptide substrate (PDB 1F8A) led us to identify Arg14, Arg17, Tyr23 and Phe25, as well as Trp34 as critical residues for the interaction with the phosphosubstrate (GWEKRMSRSSGRVYYFNHITNASQWERPSG) (Fig. 2B). We therefore synthesized a short peptide derivative of this WW domain (WWshort) which comprises these key residues in the linear order of appearance that mimicks the interface (Phe25, Arg14, Tyr23, Arg17) interspaced by small uncharged amino acids, and which ends with Trp34 followed by the same five amino acids as in the native WW domain of Pin1 (GFARVYMSRSSGWERPSG). We further synthesized a peptide comprising the WWshort peptide followed by the Rb substrate sequence (WWRb peptide). Titration experiments performed with an FITC-labelled Rb substrate peptide revealed that the WWRb peptide indeed interacted with the phosphorylated form of Rb substrate peptide with a dissociation constant value of 80 ± 37 nM, similar to the long WW peptide (118 ± 37 nM) (Fig. 2C). In comparison these peptides bound the unphosphorylated substrate peptide with significantly lower dissociation values 628 ± 109 nM and 675 ± 260 nM for the WWRb and the WWlong peptides respectively, indicating that they preferentially bind the phosphorylated substrate, as expected from a PAABD (Fig. S3). Moreover, in both cases, the WWRb peptide promoted greater fluorescence enhancement of the fluorescently-labelled Rb substrate than WWlong peptide, suggesting the WWshort sequence was better suited as a PAABD for a biosensing application. We further asked whether the Rb substrate peptide could bind the recombinant form of CDK4. Indeed the FITC-

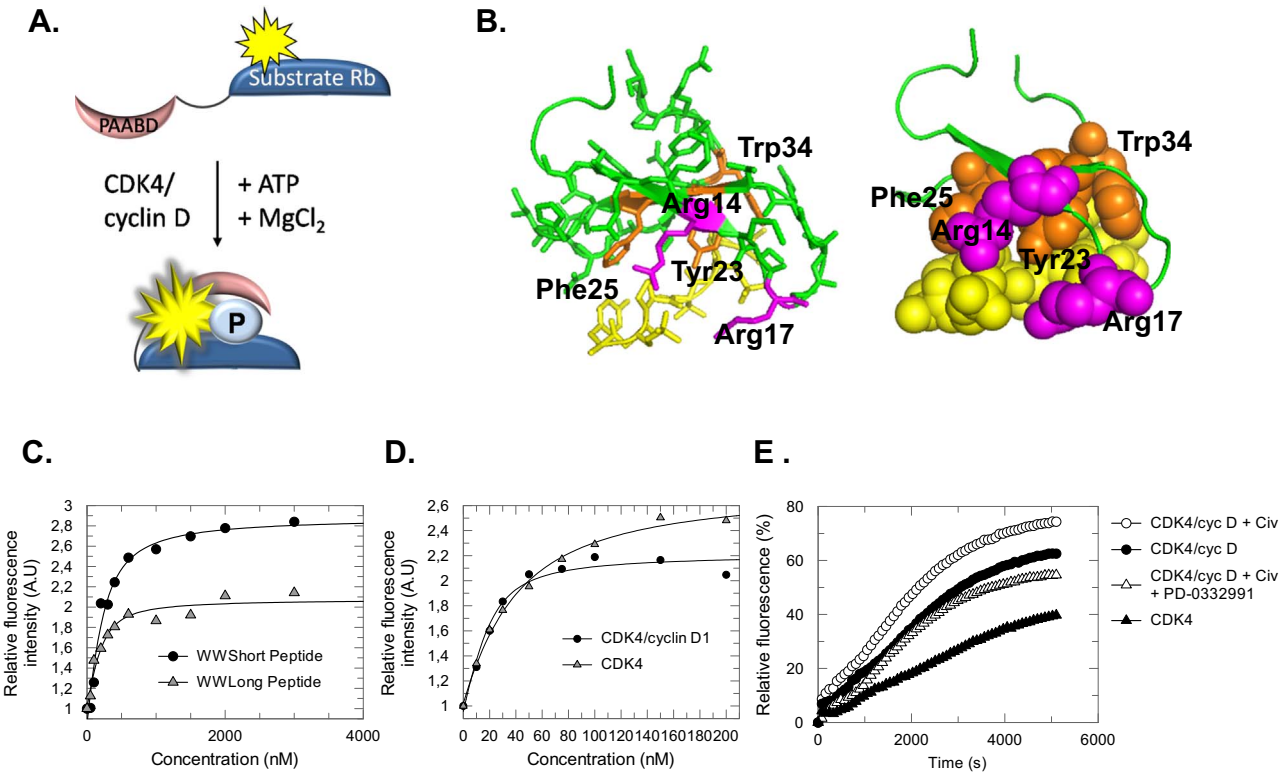

Fig. 2. Design and characterization of the CDKACT4 peptide biosensor. (A) CDKACT4 peptide biosensor consists of a substrate sequence derived from pRb (as in CDKACTRb), and a phospho amino acid-binding peptide derived from the interface of Pin1 WW domain with a phosphorylated substrate peptide. (B) The Arg, Tyr, Phe and Trp residues at interface between Pin1 WW domain (green) that recognize a phosphorylated peptide (yellow) are highlighted in pink (Arg) and orange (Tyr, Phe and Trp) (PDB 1F8A). (C) Fluorescence titration of 200 nM FITC-labelled phospho-Rb peptide with full-length WW peptide (triangles) and WWRb peptide (circles). (D) Fluorescence titration of 200 nM FITC-labelled Rb substrate peptide with monomeric GST-CDK4 (triangles) and GST-CDK4/Cyclin D1 complex (circles). (E) Fluorescence profile of 150 nM TAMRA-labelled CDKACT4 peptide biosensor incubated with 75 nM recombinant GST-CDK4 (black triangles), GST-CDK4/Cyclin D1 (black circles) or GST-CDK4/Cyclin D1 pre-incubated with the CDK-activating Kinase CIV to phosphorylate Thr172 (open circles) and with 10 μM PD-0332991 (open triangles).

labelled Rb substrate peptide bound monomeric GST-CDK4 with a dissociation constant value of 30 ± 5 nM and its affinity increased to a Kd value of 7 ± 3 nM when the kinase was complexed to Cyclin D1 (Fig. 2D), as expected from studies showing that the substrate preferentially binds the catalytic cleft of heterodimeric CDK2/Cyclin A, which is conformationally more favourable than that of monomeric CDK2 (Brown et al., 1999). The WWRb or CDKACT4 peptide biosensor was further implemented to monitor response to recombinant CDK4 kinase *in vitro* in the presence of ATP and $MgCl_2$, following labelling of the unique cysteine within the substrate sequence with TAMRA. Analysis of changes in fluorescence intensity over time revealed that monomeric CDK4 bound the biosensor, inducing fluorescence enhancement of 40%, but that the biosensor responded to CDK4/Cyclin D1 complex further, with a net increase in relative fluorescence intensity (60%). The relative increase in fluorescence reached 75% when CDK4/Cyclin D1 was preincubated with the CDK-activating kinase (to phosphorylate the activation loop), inferring that the kinase is catalytically more active in these conditions; in contrast, activity was partially reduced (55%) upon incubation with the CDK4 inhibitor PD-0332991 (Fig. 2E).

We further implemented the TAMRA-labelled CDKACT4 peptide biosensor to probe CDK4/Cyclin D kinase activity in A375 melanoma cell extracts, which resulted in a robust increase in fluorescence (similar to the enhancement profile observed with recombinant CDK4/Cyclin D1), whereas TAMRA-labelled Rb substrate peptide did not exhibit any change in fluorescence (Fig. 3A). In contrast, a Cy3 or Dylight-650-labelled CDKACT4 peptide barely responded to CDK4 activity in cell extracts, indicating that the response is associated with the sensitivity of the dye conjugated to the peptide (Fig. S4). We therefore asked whether the TAMRA-labelled CDKACT4 peptide would enable us to identify fractions bearing CDK4 activity following fractionation of A375 cell extracts by gel filtration chromatography. As shown in Fig. 3B, fractions in which Western blotting revealed the presence of CDK4 (16–18 mL) induced a significantly higher response of the peptide biosensor.

Moreover, the fluorescence of the TAMRA-CDKACT4 peptide biosensor was decreased in a dose-dependent fashion upon treatment of cells from which extracts were prepared with the CDK4 inhibitors PD-0332991 and LY2835219, but not upon addition of Roscovitine, which preferentially inhibits CDK2, CDK1, CDK5, CDK7 and CDK9 (Fig. 4A). In the absence of cell extracts neither PD-0332991, Roscovitine, LY2835219 nor DMSO had any significant effect on the fluorescence of TAMRA-CDKACT4 peptide biosensor (Fig. S5). Likewise, the biosensor reported on a reduced CDK4 activity in A375 cells treated with siRNA targeting CDK4 in which CDK4 protein levels were partially reduced (Fig. 4B). These results reveal that the CDKACT4 peptide biosensor, comprising a short artificial phosphorecognition domain derived from the WW domain of Pin1 and a substrate sequence derived from Rb, constitutes a specific and sensitive tool to quantify CDK4 activity in melanoma cell extracts following treatment with selective inhibitors or downregulation of kinase levels by RNA silencing.

We next addressed whether CDKACT4 peptide biosensor was suited to quantify differences in CDK4 hyperactivity in different cell lines. First, comparison of the biosensor response to cell extracts from healthy fibroblasts and the A375 melanoma cell line revealed a significantly greater activity in A375 cells, consistent with the lack of control of CDK4 in this cell line due to $p16^{INK4a}$ loss of function (Fig. 5A and B). We next asked whether CDKACT4 could serve to

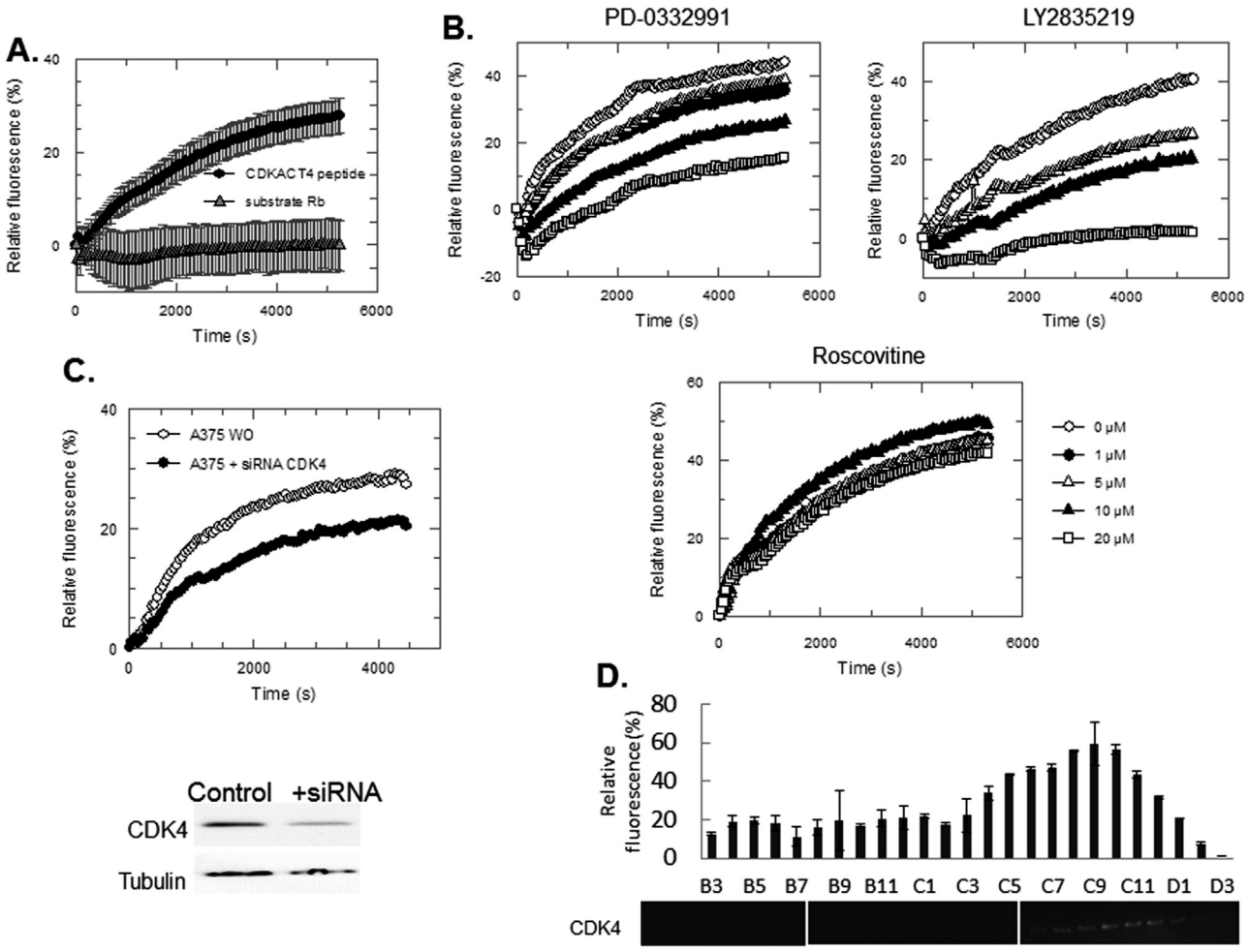

Fig. 3. Monitoring CDK4/Cyclin D activity in melanoma cell extracts. Fluorescence of 150 nM TAMRA-labelled CDKACT4 peptide biosensor was monitored over time upon incubation with (A) 40 µg A375 cell extracts (circles) and compared to the 150 nM TAMRA-labelled Rb substrate peptide alone (triangles). (B) Histogramme representation of CDK4 activity measured in 500 µL fractions of A375 cell extracts purified by gel filtration chromatography (Superose 6) and Western blot of CDK4 levels in the same fractions.

measure sensitive differences in CDK4 activity between melanoma cell lines harbouring different molecular alterations that ultimately converge on CDK4/Cyclin D activity. Specifically, CDKACT4 was incubated with normalized extracts derived from cell lines harbouring different combinations of wild-type or loss-of function $p16^{INK4a}$ (the endogenous inhibitor of CDK4), wild-type or mutated CDK4 (R24C mutation which prevents the binding of $p16^{INK4a}$), BRaf and NRas. Fluorescent profiles of the CDKACT4 peptide biosensor revealed the highest CDK4 activity in A375 (CDKN2A loss of function, BRaf V600E), Mewo (CDKN2A loss of function, Wt CDK4) and SK-MEL28 (R24C CDK4, BRaf V600E) cell lines, followed by SK-MEL2 (NRas mutation (Q61R)) (Fig. 5C and D). Quantification of the relative fluorescence intensity values at the plateau of response in a histogram clearly reveals significant differences in CDK4 activity between these cell lines (Fig. 5D). These response profiles are consistent with the genotypes of these strains in which loss of function of CDKN2A or mutation of the R24C CDK4 mutant both lead to unrestricted, constitutive activity of CDK4 in A375, SK-MEL28 and Mewo cell lines, in comparison with SK-MEL2 cell line which bears wild-type CDK4, $p16^{INK4a}$ and pRb. Importantly, the information provided by the biosensor differs from the protein expression profiles revealed by Western blotting, which do not predict any major differences in CDK4 activity between the different melanoma cell lines (Fig. 5E and F).

Taken together these experiments show that the CDKACT4 peptide biosensor is a useful tool to compare and quantify differences in CDK4/Cyclin D kinase activity between different melanoma cell lines, which cannot be identified by quantification of protein kinase expression levels alone, as they reflect mutations or molecular alterations in components of the $p16^{INK4a}$-Cyclin D-CDK4/6-pRb pathway which ultimately converge on CDK4 kinase activity.

3.3. *Quantifying CDK4/Cyclin D activity in skin biopsies and melanoma xenograft lysates*

Since the CDKACT4 peptide biosensor responded to CDK4 activity in melanoma cell extracts and reported differences between cell lines with different $p16^{INK4a}$ and CDK4 genotypes, we asked whether it could be applied to quantify CDK4 activity in skin biopsies. First, we assessed and calibrated its response to different concentrations of total healthy skin samples, relative to A375 cell extracts (Fig. 6A). As with melanoma cell extracts, CDKACT4 fluorescence was decreased by addition of PD-0332991 (Fig. 6B). We further sought to determine whether CDK4 activity could be detected in the dermis or epidermis, and found that it was essentially present in the latter (Fig. 6C), consistent with the fact that rapidly dividing cells are found in the epidermis.

Finally we asked whether CDKACT4 could be implemented to monitor subtle differences in CDK4 activity in tumour xenografts following short- and long-term administration of kinase inhibitors. To this aim, we implanted the melanoma cell line A375

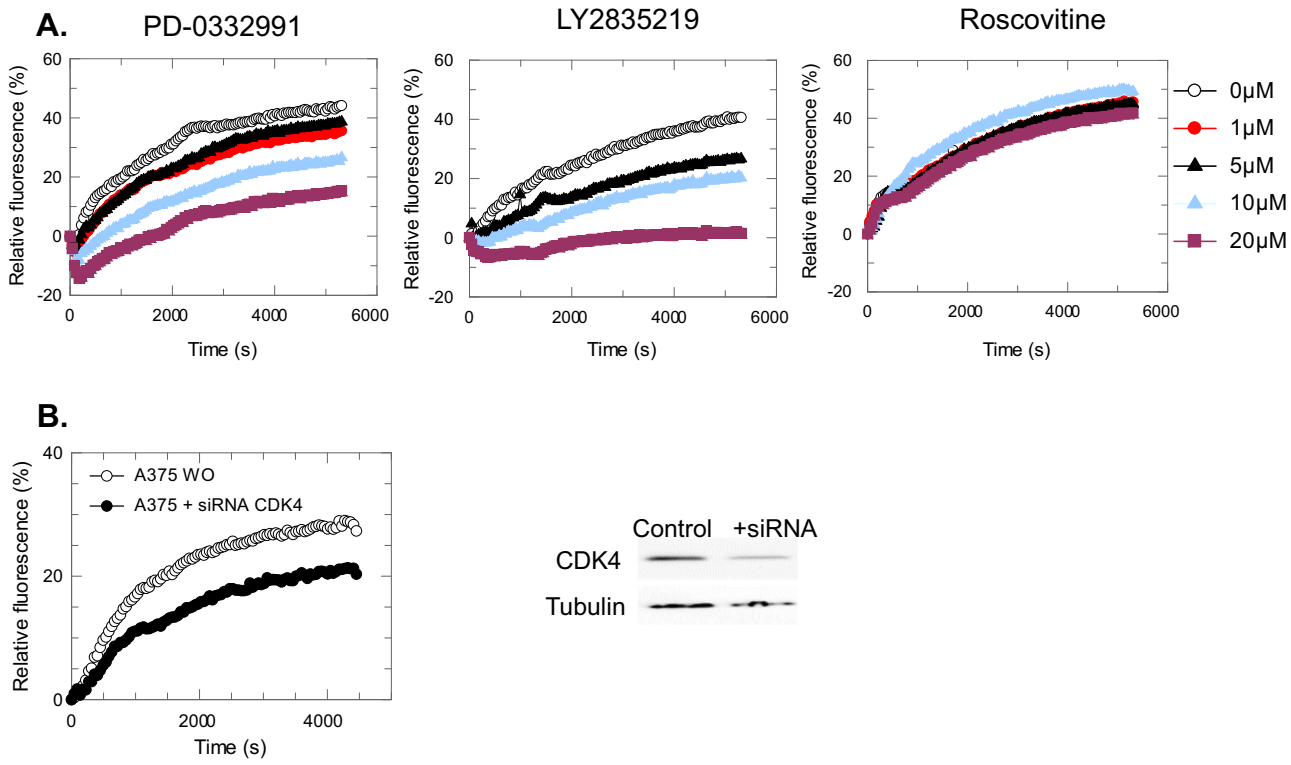

Fig. 4. Monitoring inhibition of CDK4/Cyclin D activity in melanoma cell extracts. (A) 40 µg A375 cell extracts treated with 0 µM (open circles), 1 µM (red circles), 5 µM (black triangles), 10 µM (blue triangles), 20 µM (purple squares) PD-0332991, Roscovitine or LY2835219. (B) 40 µg A375 cell extracts untreated (open circles) or treated with siRNA targeting CDK4 (black circles) and Western blot of CDK4 and tubulin protein levels from these cell extracts.

subcutaneously into the flank of nude mice and after 24 days of tumour growth, mice were treated daily either with the CDK4 inhibitor PD-0332991 at 150 mg/kg for 3 or 7 days, or with the CDK2/5/7/9 inhibitor Roscovitine at 50 mg/kg for 5 or 11 days. Following treatment with PD-0332991, we did not observe any growth inhibition of melanoma tumour xenografts compared to mock treated mice (Fig. 7A and B), nor any specific decrease in CDK4 protein levels (Fig. S6). Likewise treatment with Roscovitine had no major effect after 5 days, but significantly affected tumour growth after 11 days (Fig. 7C). Biopsies of the xenografted tumours from three mice for each of these conditions were lysed and cell extracts incubated with TAMRA-labelled CDKACT4 peptide biosensor. We further normalized the response of CDKACT4 to that of luciferase activity of the A375 xenograft lysates, to minimize any differences that might be associated with tumoral heterogeneity, and found that all samples responded in a consistent fashion (Fig. 7D and E). Indeed, these experiments revealed that 150 mg/kg PD-0332991 had no inhibitory effect on CDK4 activity after 3 days of treatment, whereas after 7 days CDK4 activity was slightly decreased. In contrast, treatment of A375 xenografted tumours with 50 mg/kg Roscovitine, whether for 5 or 11 days, had no significant effect on CDKACT4 fluorescence, although the latter treatment clearly affected tumour growth, consistent with the inhibitory action of this compound towards CDKs other than CDK4/6.

Taken together our results show that CDKACT4 peptide biosensor can be implemented to quantify CDK4/Cyclin D kinase activity in skin biopsies and melanoma xenografts, thereby reporting on CDK4 inhibition in a sensitive and specific fashion. Moreover our results demonstrate the utility of this technology to monitor inhibition of CDK4 by small molecule drugs targeting this kinase, at early stages when measurement of tumoral volumes does not yet reflect any detectable effect of these drugs.

4. Discussion

The limited efficacy of current therapeutics for treatment of melanoma and the lack of diagnostic assays to detect the onset of this disease calls for new strategies to probe relevant melanoma-specific biomarkers at an early stage and monitor their response to targeted therapeutics. The development of novel technologies is indeed essential since melanoma can be readily treated if detected at an early stage, but is incurable once it metastasizes. In particular enzymatic activities associated with dysregulated molecular signaling pathways constitute attractive biomarkers that may reflect the molecular alterations of one or several upstream regulatory partners, thereby complementing existing immunological approaches.

Fluorescent biosensors constitute potent tools for reporting on enzymatic activities in complex biological samples such as the cellular cytoplasm or the tumoral environment. Over the past decade, a wide variety of fluorescent biosensors have been developed to monitor and image enzymatic activities in living cells and have more recently proven to constitute attractive tools for biomedical applications (Lemke and Schultz, 2011). Indeed, several genetically-encoded FRET-based fluorescent biosensors have been developed to monitor aberrant kinase activity associated with cancer, such as the Bcr-Abl biosensor implemented to measure hyperactivity in cells of CML patients (Mizutani et al., 2010) or the Src biosensor applied to study spatial control of Src in pancreatic cancer by intravital FLIM-FRET imaging (Nobis et al., 2013). However, these systems require transfection and time for ectopic expression in living cells and are therefore not adapted for diagnostic assays using cell extracts or biopsies. In contrast, non-genetic fluorescent reporters based on polymeric or polypeptide scaffolds are well suited for such applications, since they can directly be incubated with enzymes or lysates containing activities to be probed, and can further be conjugated to a large choice of

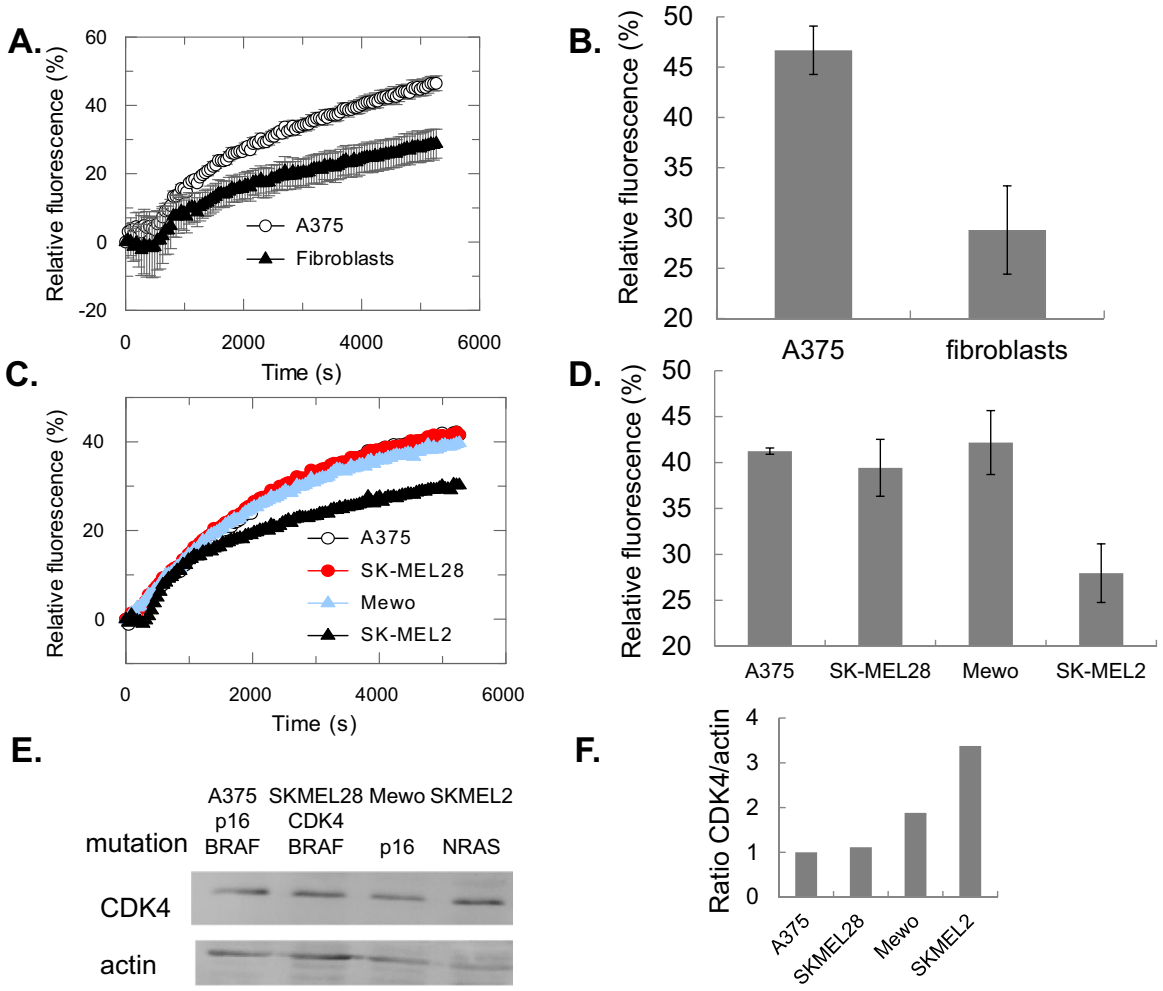

Fig. 5. Monitoring CDK4/Cyclin D activity in different melanoma cell lines. Fluorescence of 150 nM TAMRA-labelled CDKACT4 peptide biosensor was monitored over time upon incubation with (A and B) 40 μg A375 cell extracts (open circles) or fibroblasts (black triangles) (C and D) 40 μg from melanoma cell lines A375 (open circles), SK-MEL28 (red circles), Mewo (blue triangles), SK-MEL2 (black triangles). Histogramme quantifications in B and D represent relative fluorescence values of the assay at 5000 s (E) Western Blot of CDK4 levels in these different melanoma cell lines. (F) Quantification of CDK4/Actin levels.

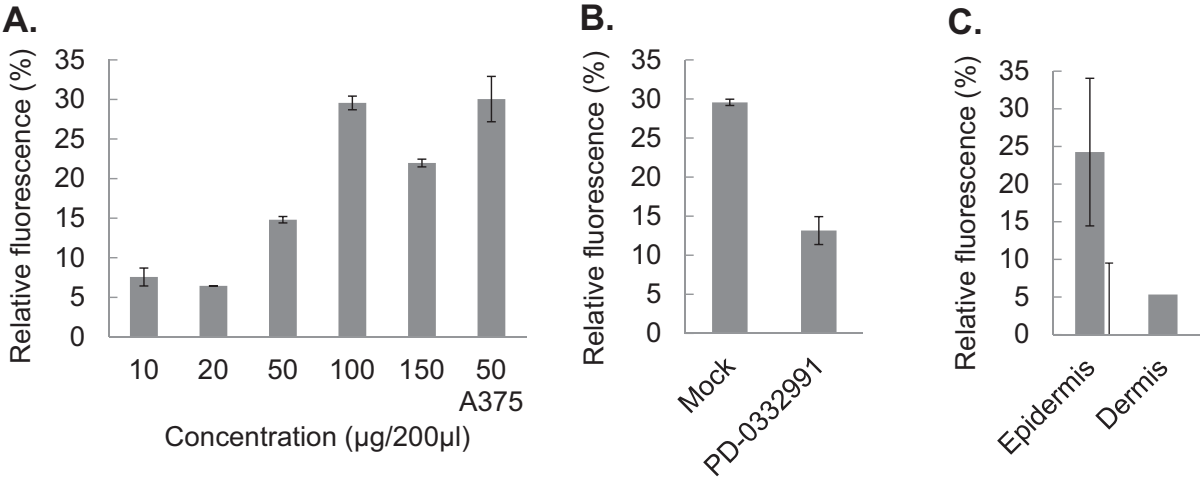

Fig. 6. Quantifying CDK4/Cyclin D activity in skin biopsies. Fluorescence of 150 nM TAMRA-labelled CDKACT4 peptide biosensor was monitored over time upon incubation with skin biopsies. Results are presented as histograms corresponding to the average of fluorescent intensity measurements at 5000 s in duplicate experiments with standard deviation bars. (A) Concentration-dependent response to healthy skin samples compared to 50 μg A375 cell extracts. (B) Inhibition of response to CDK4/Cyclin D activity upon addition of 20 μM PD-0332991 to 100 μg skin samples. (C) Differential response to 50 μg total proteins extracted from dermis *versus* epidermis.

synthetic probes, providing a controlled platform which can be readily implemented to probe specific targets of interest (Pazos et al., 2009). Several non-genetic biosensors have been engineered to monitor extracellular proteolytic activities, such as metallo-proteases secreted at the tumour site (Bogyo, 2006; Weissleder and Pittet, 2008). Moreover a wide variety of peptide biosensors

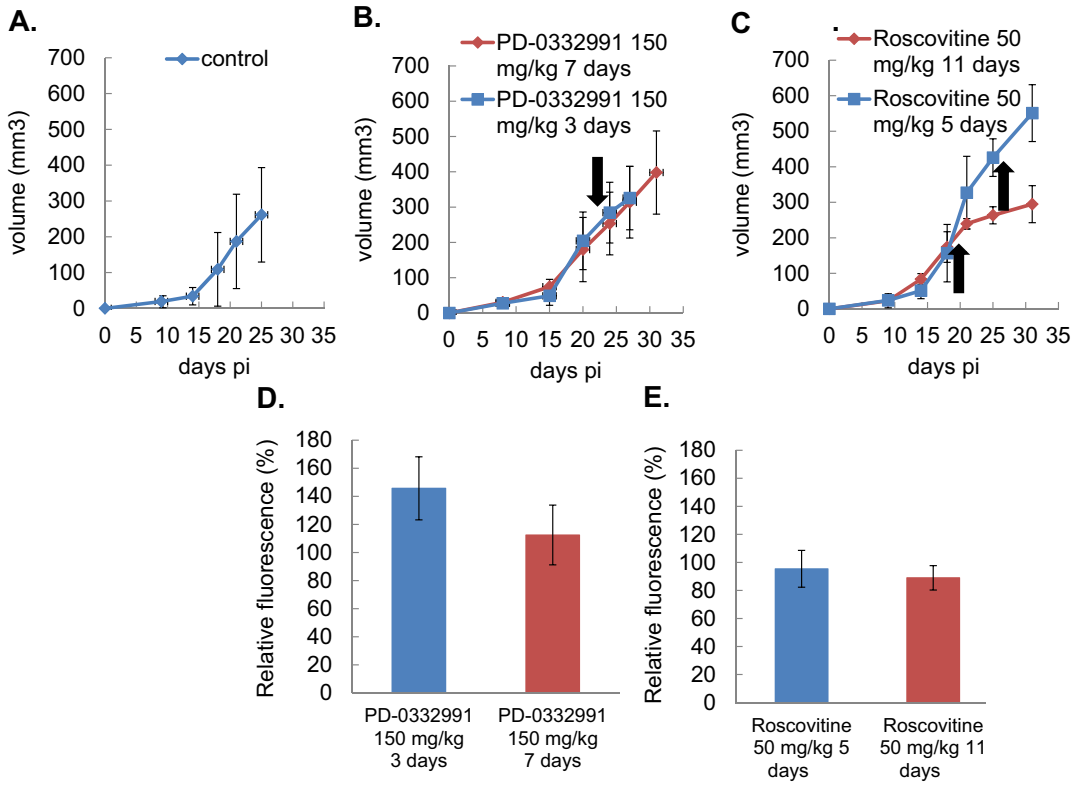

Fig. 7. Response of CDKACT4 peptide biosensor to CDK4 activity in A375 xenografts treated with PD-0332991 or Roscovitine. A375 xenografts implanted in mice were treated with 150 mg/kg PD-0332991 for 3 or 7 days or 50 mg/kg Roscovitine for 5 or 11 days. Growth curves of (A) mock-treated (control) (B) PD-0332991-treated, or (C) Roscovitine-treated xenografts. Arrows indicate time of treatment. (D) Fluorescence response of 150 nM TAMRA-labelled CDKACT4 peptide biosensor to 100 μL total proteins extracted from A375 tumour xenografts treated with PD-0332991, normalized to luciferase activity measured in the same samples (E) Fluorescence response of 150 nM TAMRA-labelled CDKACT4 peptide biosensor to 100 μL total proteins extracted from A375 tumour xenografts treated with Roscovitine, normalized as described in (D). Histograms represent experiments performed in duplicate from three mice for each condition and relative to control (mock-treated) tumour samples.

have been developed to probe protein kinase activities (González-Vera, 2012; Nhu Ngoc Van and Morris, 2013). These include peptide biosensors conjugated to solvatochromic probes, which respond either directly to proximal phosphorylation within the substrate sequence of the biosensor by kinases such as PKA, PKC, ERK, Bcr-Abl, Lyn and Abl (Chen et al., 2002; Damayanti et al., 2013; Luković et al., 2009; Shults et al., 2005; Wang et al., 2010), or indirectly following interactions with phosphorecognition domains that alter biosensor fluorescence, or through quenching/unquenching strategies (Sharma et al., 2007; Wang et al., 2006; Wang and Lawrence, 2005). The recent implementation of fluorescent peptide biosensors to monitor kinase activities in cell extracts offers promising perspectives. However, to date, none of these chemical tools has been applied to quantify kinase activities in skin or tumour biopsies.

CDK4/Cyclin D kinase constitutes an established biomarker and pharmacological target in melanoma, hyperactivity of which is associated with mutations in the $p16^{INK4a}$-Cyclin D-CDK4/6-pRb pathway. Here we report on a new fluorescent biosensor, which constitutes a potent tool for probing CDK4 activity in cell extracts, skin biopsies and melanoma xenograft lysates, thereby providing a scaled and predictive readout of this enzymatic cancer biomarker. Besides being the first CDK4-specific biosensor, this bipartite peptide offers a novel and original design comprising a substrate sequence derived from Rb and an artificial phosphorecognition motif derived from the interface of a WW domain, designed through careful analysis of the structural model of the WW domain of Pin1 complexed with a phosphopeptide substrate. Since this biosensor responds to CDK4 activity through changes in fluorescence intensity, it offers a straightforward and sensitive means of monitoring kinase activity in a continuous fluorescence-based assay over time. We show here that CDKACT4 is well suited to quantify differences in CDK4 activity in lysates from different cell lines, thereby reporting on hyperactivity that cannot be identified by Western blot analysis of protein kinase expression levels, associated with multiple molecular alterations that converge on CDK4 kinase activity. It therefore constitutes a promising tool for diagnostic and prognostic purposes by affording means of monitoring cancer-associated alterations in kinase activity which are complementary to immunological identification of melanoma-specific biomarkers. Moreover this biosensor allows to quantify response to CDK4 inhibitors in cell extracts, as well as in skin biopsies and in melanoma xenograft lysates, providing a direct readout of their efficacy in a fluorescence-based assay, and thereby offering promising perspectives for developing a companion assay to assess disease progression and response to therapeutics.

5. Conclusions

Uncontrolled proliferation of melanocytes results in melanoma, the most aggressive form of skin cancer, which further metastasizes into a deadly form of cancer. Although antibody-based approaches are currently implemented for detection of several histological and serological melanoma-specific biomarkers, new tools are required to monitor enzymatic biomarkers whose hyperactivity is associated with the onset and progression of this disease. In this respect, CDK4 kinase constitutes an attractive biomarker, since the $p16^{INK4a}$-Cyclin D-CDK4/6-pRb pathway is dysregulated in 90% of melanomas, resulting in CDK4 hyperactivity,

which promotes and sustains uncontrolled cell proliferation.

Our work highlights the development of an original peptide-based fluorescent biosensor to monitor cancer-associated alterations in CDK4 kinase activity, which constitutes a versatile tool for application in cell extracts, skin biopsies and melanoma xenografts. CDKACT4 biosensor is not only the first fluorescent peptide biosensor to report on CDK4 kinase activity, it also constitutes an innovative design that incorporates a novel and artificial phosphoaminoacid recognition sequence with a CDK4-specific substrate sequence derived from Rb. Moreover this is the first fluorescent peptide biosensor which has been successfully applied to monitor kinase activities in skin samples and tumour xenografts, thereby providing functional information which will be useful to complement morphological and histological analysis of clinical samples.

CDKACT4 biosensor constitutes a first-of-a kind tool for detection of a relevant enzymatic biomarker in melanoma, and we anticipate it will enable development of a predictive diagnostic assay for detection of melanoma onset in precancerous lesions. Our study therefore emphasizes the potency of fluorescent biosensors to report and quantify enzymatic activities as an alternative to antibody-based approaches for diagnostic purposes. Furthermore we have shown that implementation of CDKACT4 constitutes a useful companion assay to identify CDK4 inhibitors which present a relevant therapeutic indication in melanoma.

Acknowledgements

This work was supported by the CNRS (Centre National de la Recherche Scientifique) and grants from the Region Languedoc-Roussillon (Grant no. DGA4/DESR/2010 Q-013) (Subvention “Chercheuse d’Avenir” 2009) and Institut de Recherche contre Cancer (INCA FOLDLUNGK4 No 2015-043) to MCM. CP was supported by a fellowship from the CBS2 doctoral school of Montpellier University. JAGV was supported by a Marie-Curie fellowship EC-FP7 Framework (PIEF-GA-2013–623151). We thank Carmen-Mihaela Tîlmaciu for critical reading of the manuscript.

Appendix A. Supplementary material

Supplementary data associated with this article can be found in the online version at http://dx.doi.org/10.1016/j.bios.2016.04.050.

References

Anai, T., Nakata, E., Koshi, Y., Ojida, A., Hamachi, I., 2007. J. Am. Chem. Soc. 129, 6232–6239.
Bogyo, M., 2006. Nat. Chem. Biol. 2, 229–230.
Bosserhoff, A.K., Kaufmann, M., Kaluza, B., Bartke, I., Zirngibl, H., Hein, R., Stolz, W., Buettner, R., 1997. Cancer Res. 57, 3149–3153.
Brown, N.R., Noble, M.E., Lawrie, A.M., Morris, M.C., Tunnah, P., Divita, G., Johnson, L. N., Endicott, J.A., 1999. J. Biol. Chem. 274, 8746–8756.
Cancer Genome Atlas Network, 2015. Cell 161, 1681–1696.
Chawla, R., Procknow, J.A., Tantravahi, R.V., Khurana, J.S., Litvin, J., Reddy, E.P., 2010. Cell Cycle 9, 3305–3314.
Chen, C.-A., Yeh, R.-H., Lawrence, D.S., 2002. J. Am. Chem. Soc. 124, 3840–3841.
Crombez, L., Aldrian-Herrada, G., Konate, K., Nguyen, Q.N., McMaster, G.K., Brasseur, R., Heitz, F., Divita, G., 2009. Mol. Ther. 17, 95–103.
Damayanti, N.P., Parker, L.L., Irudayaraj, J.M.K., 2013. Angew. Chem. Int. Ed. 52, 3931–3934.
Gondeau, C., Gerbal-Chaloin, S., Bello, P., Aldrian-Herrada, G., Morris, M.C., Divita, G., 2005. J. Biol. Chem. 280, 13793–13800.
González-Vera, J.A., 2012. Chem. Soc. Rev. 41, 1652–1664.
Grafstrom, R.H., Pan, W., Hoess, R.H., 1999. Carcinogenesis 20, 193–198.
Guo, H.B., Stoffel-Wagner, B., Bierwirth, T., Mezger, J., Klingmüller, D., 1995. Eur. J. Cancer 31A, 924–928.
Hodis, E., Watson, I.R., Kryukov, G.V., Arold, S.T., Imielinski, M., Theurillat, J.-P., Nickerson, E., Auclair, D., Li, L., Place, C., Dicara, D., Ramos, A.H., Lawrence, M.S., Cibulskis, K., Sivachenko, A., Voet, D., Saksena, G., Stransky, N., Onofrio, R.C., Winckler, W., Ardlie, K., Wagle, N., Wargo, J., Chong, K., Morton, D.L., Stemke-Hale, K., Chen, G., Noble, M., Meyerson, M., Ladbury, J.E., Davies, M.A., Gershenwald, J.E., Wagner, S.N., Hoon, D.S.B., Schadendorf, D., Lander, E.S., Gabriel, S.B., Getz, G., Garraway, L.A., Chin, L., 2012. Cell 150, 251–263.
Lemke, E.A., Schultz, C., 2011. Nat. Chem. Biol. 7, 480–483.
Lozano, R., Naghavi, M., Foreman, K., Lim, S., Shibuya, K., Aboyans, V., Abraham, J., Adair, T., Aggarwal, R., Ahn, S.Y., Alvarado, M., Anderson, H.R., Anderson, L.M., Andrews, K.G., Atkinson, C., Baddour, L.M., Barker-Collo, S., Bartels, D.H., Bell, M. L., Benjamin, E.J., Bennett, D., Bhalla, K., Bikbov, B., Bin Abdulhak, A., Birbeck, G., Blyth, F., Bolliger, I., Boufous, S., Bucello, C., Burch, M., Burney, P., Carapetis, J., Chen, H., Chou, D., Chugh, S.S., Coffeng, L.E., Colan, S.D., Colquhoun, S., Colson, K. E., Condon, J., Connor, M.D., Cooper, L.T., Corriere, M., Cortinovis, M., de Vaccaro, K.C., Couser, W., Cowie, B.C., Criqui, M.H., Cross, M., Dabhadkar, K.C., Dahodwala, N., De Leo, D., Degenhardt, L., Delossantos, A., Denenberg, J., Des Jarlais, D.C., Dharmaratne, S.D., Dorsey, E.R., Driscoll, T., Duber, H., Ebel, B., Erwin, P.J., Espindola, P., Ezzati, M., Feigin, V., Flaxman, A.D., Forouzanfar, M.H., Fowkes, F.G.R., Franklin, R., Fransen, M., Freeman, M.K., Gabriel, S.E., Gakidou, E., Gaspari, F., Gillum, R.F., Gonzalez-Medina, D., Halasa, Y.A., Haring, D., Harrison, J. E., Havmoeller, R., Hay, R.J., Hoen, B., Hotez, P.J., Hoy, D., Jacobsen, K.H., James, S. L., Jasrasaria, R., Jayaraman, S., Johns, N., Karthikeyan, G., Kassebaum, N., Keren, A., Khoo, J.-P., Knowlton, L.M., Kobusingye, O., Koranteng, A., Krishnamurthi, R., Lipnick, M., Lipshultz, S.E., Ohno, S.L., Mabweijano, J., MacIntyre, M.F., Mallinger, L., March, L., Marks, G.B., Marks, R., Matsumori, A., Matzopoulos, R., Mayosi, B. M., McAnulty, J.H., McDermott, M.M., McGrath, J., Mensah, G.A., Merriman, T.R., Michaud, C., Miller, M., Miller, T.R., Mock, C., Mocumbi, A.O., Mokdad, A.A., Moran, A., Mulholland, K., Nair, M.N., Naldi, L., Narayan, K.M.V., Nasseri, K., Norman, P., O'Donnell, M., Omer, S.B., Ortblad, K., Osborne, R., Ozgediz, D., Pahari, B., Pandian, J.D., Rivero, A.P., Padilla, R.P., Perez-Ruiz, F., Perico, N., Phillips, D., Pierce, K., Pope, C.A., Porrini, E., Pourmalek, F., Raju, M., Ranganathan, D., Rehm, J.T., Rein, D.B., Remuzzi, G., Rivara, F.P., Roberts, T., De León, F.R., Rosenfeld, L.C., Rushton, L., Sacco, R.L., Salomon, J.A., Sampson, U., Sanman, E., Schwebel, D.C., Segui-Gomez, M., Shepard, D.S., Singh, D., Singleton, J., Sliwa, K., Smith, E., Steer, A., Taylor, J.A., Thomas, B., Tleyjeh, I.M., Towbin, J.A., Truelsen, T., Undurraga, E.A., Venketasubramanian, N., Vijayakumar, L., Vos, T., Wagner, G. R., Wang, M., Wang, W., Watt, K., Weinstock, M.A., Weintraub, R., Wilkinson, J. D., Woolf, A.D., Wulf, S., Yeh, P.-H., Yip, P., Zabetian, A., Zheng, Z.-J., Lopez, A.D., Murray, C.J.L., AlMazroa, M.A., Memish, Z.A., 2012. Lancet 380, 2095–2128.
Luković, E., Vogel Taylor, E., Imperiali, B., 2009. Angew. Chem. Int. Ed. 48, 6828–6831.
Mahgoub, T., Eustace, A.J., Collins, D.M., Walsh, N., O'Donovan, N., Crown, J., 2015. Int. J. Oncol. 47, 900–908.
Malumbres, M., Barbacid, M., 2009. Nat. Rev. Cancer 9, 153–166.
Miller, D.M., Flaherty, K.T., 2014. Pigment Cell Melanoma Res. 27, 351–365.
Mizutani, T., Kondo, T., Darmanin, S., Tsuda, M., Tanaka, S., Tobiume, M., Asaka, M., Ohba, Y., 2010. Clin. Cancer Res. 16, 3964–3975.
Nhu Ngoc Van, T., Morris, M.C., 2013. Prog. Mol. Biol. Transl. Sci. 113, 217–274.
Nobis, M., McGhee, E.J., Morton, J.P., Schwarz, J.P., Karim, S.A., Quinn, J., Edward, M., Campbell, A.D., McGarry, L.C., Evans, T.R.J., Brunton, V.G., Frame, M.C., Carragher, N.O., Wang, Y., Sansom, O.J., Timpson, P., Anderson, K.I., 2013. Cancer Res. 73, 4674–4686.
Pazos, E., Vázquez, O., Mascareñas, J.L., Vázquez, M.E., 2009. Chem. Soc. Rev. 38, 3348–3359.
Quast, S.-A., Steinhorst, K., Plötz, M., Eberle, J., 2015. J. Invest. Dermatol.
Sharma, V., Agnes, R.S., Lawrence, D.S., 2007. J. Am. Chem. Soc. 129, 2742–2743.
Sheppard, K.E., McArthur, G.A., 2013. Clin. Cancer Res. 19, 5320–5328.
Shults, M.D., Janes, K.A., Lauffenburger, D.A., Imperiali, B., 2005. Nat. Methods 2, 277–283.
Taylor, C.R., 2000. Arch. Pathol. Lab. Med. 124, 945–951.
Tsao, H., Chin, L., Garraway, L.A., Fisher, D.E., 2012. Genes Dev. 26, 1131–1155.
Utikal, J., Schadendorf, D., Ugurel, S., 2007. Arch. Dermatol. Res. 298, 469–477.
Van, T.N.N., Pellerano, M., Lykaso, S., Morris, M.C., 2014. Chembiochem.
Wang, Q., Lawrence, D.S., 2005. J. Am. Chem. Soc. 127, 7684–7685.
Wang, Q., Dai, Z., Cahill, S.M., Blumenstein, M., Lawrence, D.S., 2006. J. Am. Chem. Soc. 128, 14016–14017.
Wang, Q., Zimmerman, E.I., Toutchkine, A., Martin, T.D., Graves, L.M., Lawrence, D.S., 2010. ACS Chem. Biol. 5, 887–895.
Weissleder, R., Pittet, M.J., 2008. Nature 452, 580–589.
Young, R.J., Waldeck, K., Martin, C., Foo, J.H., Cameron, D.P., Kirby, L., Do, H., Mitchell, C., Cullinane, C., Liu, W., Fox, S.B., Dutton-Regester, K., Hayward, N.K., Jene, N., Dobrovic, A., Pearson, R.B., Christensen, J.G., Randolph, S., McArthur, G.A., Sheppard, K.E., 2014. Pigment Cell Melanoma Res. 27, 590–600.